

Effect of different alkali metal cations on the oxygen evolution activity and battery capacity of nickel electrodes in concentrated hydroxide electrolytes

Mangel Raventos, A.; Kortlever, R.

DOI

[10.1016/j.electacta.2022.140255](https://doi.org/10.1016/j.electacta.2022.140255)

Publication date

2022

Document Version

Final published version

Published in

Electrochimica Acta

Citation (APA)

Mangel Raventos, A., & Kortlever, R. (2022). Effect of different alkali metal cations on the oxygen evolution activity and battery capacity of nickel electrodes in concentrated hydroxide electrolytes. *Electrochimica Acta*, 415, Article 140255. <https://doi.org/10.1016/j.electacta.2022.140255>

Important note

To cite this publication, please use the final published version (if applicable). Please check the document version above.

Copyright

Other than for strictly personal use, it is not permitted to download, forward or distribute the text or part of it, without the consent of the author(s) and/or copyright holder(s), unless the work is under an open content license such as Creative Commons.

Takedown policy

Please contact us and provide details if you believe this document breaches copyrights. We will remove access to the work immediately and investigate your claim.



Effect of different alkali metal cations on the oxygen evolution activity and battery capacity of nickel electrodes in concentrated hydroxide electrolytes

A. Mangel Raventos, R. Kortlever*

Department of Process and Energy, Mechanical, Maritime and Materials Engineering, Delft University of Technology, Delft, the Netherlands

ARTICLE INFO

Keywords:

Battery
Alkaline electrolysis
OER
Electrocatalysis
Energy storage

ABSTRACT

The effect of different alkali metal cations on the oxygen evolution activity and battery capacity of nickel electrodes has recently been studied in low concentration alkali hydroxide electrolytes. As high concentration hydroxide electrolytes are favored in applications due to their high conductivity, we investigate if the cation effects observed in low concentration electrolytes translate to more industrially relevant conditions for both alkaline water electrolysis and nickel iron batteries. We investigate the alkali metal cation effect on the electrochemical properties of nickel electrodes in highly concentrated hydroxide electrolytes by adding Li^+ , Na^+ , Cs^+ and Rb^+ cations to a 6.5 M KOH electrolyte, while keeping the hydroxide concentration constant. For OER we find a trend in activity similar to that at low concentrations $\text{Rb}^+ > \text{Cs}^+ > \text{K}^+ > \text{Na}^+ > \text{Li}^+$, where especially larger additions of Rb^+ and Cs^+ (1 M or 0.5 M) cause a significant decrease in OER potential. Smaller cations interact with the layered hydroxide structures in NiOOH to stabilize the α/γ phases and increase the potential for OER. The intercalation of small cations also causes an increase in battery electrode capacity because of the higher average valence of the Ni(OH)₂/NiOOH α/γ pair. Small concentrations of Li^+ added to a concentrated KOH electrolyte can therefore be beneficial for the nickel electrode battery functionality and for an integrated battery and electrolyser system, where it increases the battery capacity without a significant increase in OER onset potential.

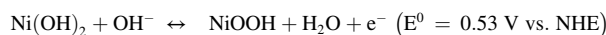
1. Introduction

An increase in both global population and energy demand, together with a rising percentage of renewable energy sources on the grid, demand an increase in energy storage capacity [1–3]. Electrochemical storage techniques will play a key role in the energy transition to cleaner and more sustainable energy forms [4–6].

Batteries have a high energy efficiency and high roundtrip efficiency, but are not ideal for longer term storage due to self-discharge and costs. Water electrolysis can be advantageous for longer term, seasonal storage as the hydrogen that is produced can be stored for prolonged periods of time [7]. Battery storage and water electrolysis can also be integrated in a single device to provide both long-term and short-term storage capacity [7]. The battolyser, an integrated battery and electrolyser device, combines two different energy storage functionalities: a nickel-iron battery and an alkaline electrolyser [8,9]. Electricity can be stored and generated from the materials in the electrodes via the Ni(OH)₂/NiOOH and Fe(OH)₂/Fe redox couples [10]. When the maximum battery capacity is reached, the battolyser makes use of the electrocatalytic

properties of Fe and NiOOH for electrochemical hydrogen and oxygen evolution and the device acts as an alkaline electrolyser. Thereby, the excess electricity that cannot be stored in the battery functionality is used to split water molecules from the electrolyte, generating hydrogen and oxygen [7,11]. The relevant reactions on both the nickel and iron electrode are given below, alongside their standard equilibrium potential (E^0):

Ni electrode:



Fe electrode:



The development and evaluation of different catalysts for the oxygen

* Corresponding author.

E-mail address: R.Kortlever@tudelft.nl (R. Kortlever).

evolution reaction (OER) has been the subject of a considerable amount of research in recent years. Nickel oxyhydroxide layered double hydroxides (NiOOH-LDH) are promising materials for OER in alkaline conditions because of their excellent catalytic performance and lower costs compared to other good electrocatalytic materials, such as IrO_2 and RuO_2 [12]. Nonetheless, most experimental studies have used dilute electrolyte solutions to study these electrocatalysts, even though the pH of the electrolyte solution is known to affect the catalytic properties of NiOOH materials and industrial applications make use of highly concentrated electrolytes [13,14].

Studies focusing on electrolyte effects have shown that cations can intercalate into the $\text{Ni}(\text{OH})_2$ layered structure and thereby modify its electrocatalytic performance [15,16]. Constantin et al. report a modification in the hydroxide layers leading to an increase in the catalytic activity of OER on NiOOH in the presence of Li^+ [17]. The intercalation of Cs^+ cations has been shown to elongate Ni-O bonds because of their larger size [18,19]. Garcia et al. report that the OER activity of NiOOH in alkali hydroxide electrolytes follows the trend $\text{Cs}^+ > \text{Na}^+ > \text{K}^+ > \text{Li}^+$. Using surface enhanced Raman spectroscopy (SERS) they show that the presence of cations affects the formation of the superoxo OER intermediate ($\text{Ni}-\text{OO}^-$). The cations interact with the $\text{Ni}-\text{OO}^-$ species, forming a $\text{NiOO}^- - \text{M}^+$ species that is stabilized by bigger cations, such as Cs^+ . The $\text{NiOO}^- - \text{M}^+$ species then serve as a precursor to OER [20]. This indicates that alkali metal cations have a significant effect on OER activity of NiOOH and therefore can be used to tune the reactivity of the catalytic surface [18]. However, all of these effects have solely been reported in low concentration electrolytes, typically using a 0.1 M alkali hydroxide electrolyte, and therefore there is little insight on how these processes affect alkaline electrolysis in more industrially relevant, concentrated alkali hydroxide electrolytes.

Moreover, the presence of alkali cations in the electrolyte has a substantial effect on NiFe battery operation. Typically, LiOH is added to KOH electrolytes in NiFe batteries to increase the lifetime and cycleability of the batteries [21]. Specifically, the addition of LiOH has been shown to increase the lifetime of the positive $\text{Ni}(\text{OH})_2$ electrode [10], as at temperatures above 40 °C Fe can dissolve into the concentrated KOH electrolyte and migrate towards the positive Ni electrode. This leads to Fe inclusions in the Ni electrode that can stabilize the NiOOH α/γ phase, leading to a lower onset potential for OER [22]. Fe has been reported to intercalate into $\text{Ni}(\text{OH})_2$ after only 5 cyclic voltammetry cycles, resulting in larger intersheet spacing in the $\text{NiFe}(\text{OH})_2$ structure [23]. This in turn causes a shift in potential for the $\text{Ni}(\text{OH})_2/\text{NiOOH}$ redox couple and a reduction in the onset potential for OER. These alterations result in a higher electron capacity for battery storage due to the higher average valence of the $\text{Ni}(\text{OH})_2/\text{NiOOH}$ α/γ pair and a higher loss due to the secondary oxygen evolution reaction [24–26].

Here, we investigate the effect of concentrated alkali hydroxide electrolyte mixtures on the OER performance and battery functionality of nickel electrodes. We do this by adding specific concentrations of alkali cations, namely Li^+ , Na^+ , Cs^+ and Rb^+ , to highly concentrated KOH electrolytes and performing both rotating disk electrode (RDE) and battery cycling experiments. Moreover, we optimize the electrolyte composition for the integration of both the NiFe battery and alkaline electrolysis functionalities in a hybrid device such as the battolyser. For OER we find a trend in activity similar to that at low concentrations $\text{Rb}^+ > \text{Cs}^+ > \text{K}^+ > \text{Na}^+ > \text{Li}^+$, where especially larger additions of Rb^+ and Cs^+ (1 M or 0.5 M) cause a significant decrease in OER potential. Smaller cations interact with the layered hydroxide structures in NiOOH to stabilize the α/γ phases. The intercalation of small cations also causes an increase in battery electrode capacity because of the higher average valence of the $\text{Ni}(\text{OH})_2/\text{NiOOH}$ α/γ pair. Small concentrations of Li^+ added to a concentrated KOH electrolyte can therefore be beneficial for the nickel electrode battery functionality and for an integrated battery and electrolyser system, where it increases the battery capacity without a significant increase in OER onset potential.

2. Experimental methods

2.1. Electrode preparation for RDE experiments

5 mm diameter, 4 mm thick Sigradur G glassy carbon (GC) mirror polished disks (HTW Hochtemperatur-Werkstoff GmbH) were used as working electrode substrates. To clean the electrodes, the GC disks were sonicated for 10 min each in ultrapure water, acetone, isopropanol, and again in ultrapure water.

The drop-casting procedure used in this study is based on a literature procedure [27,28]. Powder-based inks were made using the active material of the commercial battery electrodes (Ironcore Batteries, patent nr. US20140377626A1), using 3.8 mL ultrapure water (MilliQ), 1.0 ml 2-propanol (≥ 98 technical grade, VWR Chemicals), 40 μl of 5% Nafion 117 solution (Sigma Aldrich), and 80 mg of the active battery material powder. The metal oxide powder contains impurities and graphitic carbon included in the battery for additional conductivity. Characterization of the commercial electrode materials using ICP-OES results are presented in the SI, Table S.2. The inks were sonicated for 15 min after which 10 μl of catalyst ink was drop-cast onto the mirror-polished GC disk and subsequently dried in an oven at 60 °C for 10 min.

2.2. Electrolyte preparation

Experiments were performed in electrolytes with a 6.5 M hydroxide ion concentration prepared from high-purity LiOH (99.995% trace metals basis, Sigma-Aldrich), NaOH (99.99% trace metals basis, Sigma-Aldrich), KOH (99.99% trace metals basis Sigma-Aldrich), CsOH ($\geq 99.5\%$, Sigma-Aldrich) and RbOH (99%, Sigma-Aldrich). MilliQ ultrapure water (18 M Ω) was used to prepare the electrolytes. The electrolyte consisted of either pure KOH or KOH with a MOH additive, where M is either Li^+ , Na^+ , Cs^+ , or Rb^+ . The concentration of KOH and MOH is varied in accordance to Table 1, while keeping the total OH^- concentration constant, resulting in a total of 17 different electrolyte compositions being tested.

2.3. Rotating disk electrode (RDE) measurements

The GC working electrodes were mounted on a RDE assembly (Pine MSR) and cyclic voltammograms (CVs) were recorded in a three electrode cell using a Biologic VSP-300 potentiostat. A literature methodology for testing OER catalysts was used for the RDE experiments to obtain reproducible results [29]. Prior to the electrochemical measurements, the electrolyte solution was purged with O_2 for 30 min. During the CV measurements the cell was kept blanketed under O_2 by applying an O_2 flow over the electrolyte. A schematic representation of the RDE assembly is presented in Fig. S.4 in the SI.

A three electrode cell configuration with an Ag/AgCl reference electrode (Orignalys, sat. KCl) and a carbon rod counter electrode (99.999%, Strem Chemicals) was used for all electrochemical tests. All potentials were converted from the Ag/AgCl scale to the reversible hydrogen electrode (RHE) scale and are reported as such. The ohmic drop was measured using Potentiostatic Electrochemical Impedance

Table 1

Electrolyte composition variations used in this study. The total hydroxide concentration is kept constant at 6.5 M, while different alkali hydroxides ($M = \text{Li}, \text{Na}, \text{Cs}, \text{Rb}$) are mixed with KOH.

| KOH | MOH |
|--------|--------|
| 5.5 M | 1 M |
| 6 M | 0.5 M |
| 6.4 M | 0.1 M |
| 6.45 M | 0.05 M |

Spectroscopy (PEIS) with a 20 mV amplitude and CV measurements and corrected for at 85% using the Biologic EC-Lab software. The additional ohmic drop was compensated for manually. CV scans were recorded from 0.7 to 1.7 V vs. RHE for 5 cycles at 1600 rpm with a scan rate of 20 mV s⁻¹. The charge of the nickel oxide reduction peak was used to calculate the total amount of active material drop-cast on the electrodes. Consequently, all of the CVs are plotted with respect to the mass (in mg) of active material present on the electrodes for the sake of accurate comparison.

2.4. Battery cycling

A BioLogic BCS-815 Battery cycler was used to run the charge/discharge cycles on commercial NiFe batteries (Ironcore Batteries). Galvanostatic charge/discharge cycles were performed with a potential limitation of 1.1 V to avoid over-discharging.

First, thirty battery conditioning cycles were performed on each battery using a 5 M KOH (85% Sigma Aldrich) solution as electrolyte. The rated capacity of these batteries is 10Ah. The charge/discharge cycles were performed using a recommended charging rate of C/5 and a discharge rate of C/6.6. This coincides with a constant current of 2 A during charging and -1.5 A during discharge. The long-term battery experiments were performed in a highly resistant plastic enclosure, namely the cell where the commercial batteries are sold. This ensures that the experiments are performed in highly alkaline resistant cells. The electrolyte level was kept above the minimum by manual inspection and addition of MilliQ ultrapure water when necessary. After the conditioning phase the electrolyte composition was varied as shown in Table 2. Thirty galvanostatic charge/discharge cycles were performed at the same charge and discharge rate as mentioned before.

3. Results and discussion

3.1. Rotating disk electrode measurements

The effect of different cations on both the battery and the electrolysis reactions can be seen in cyclic voltammetry (CV) scans using a RDE setup. A detailed schematic of the setup is shown in Fig. S.4 of the SI. The electrode material is dropcasted using a binder, which can result in (partial) coverage of the active material by the binder itself. Additionally, during the CV experiments, some of the dropcasted material can detach from the electrode surface due to bubble formation. This makes it difficult to relate the amount of electrode material dropcasted on the GC electrode to the actual amount of active material. To provide a comparable measurement between different electrolyte compositions, the total amount of active material is calculated using the total charge of the nickel hydroxide reduction peak.

Four different concentrations of each alkali cation in KOH were tested, and the results of the experiments with the highest MOH concentrations (1.0 M MOH + 5.5 M KOH) are shown in Fig. 1. The total data set of cyclic voltammograms with different MOH concentrations is included in Fig. S.1 of the SI. Although iron incorporations in the nickel material will affect the electrochemical performance of the anode, they are considered to be uniform across all measurements as the electrode material contains 0.1 wt-% iron (see Table S.2). Therefore we hypothesize that iron inclusions from electrolyte impurities will have a negligible effect.

On the basis of the CVs shown in Fig. 1, we can determine the effect

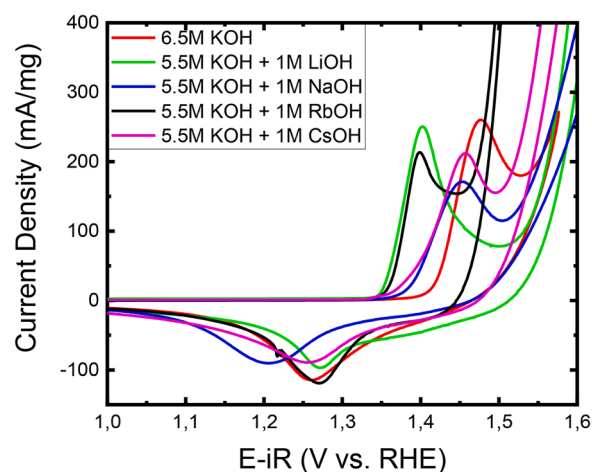


Fig. 1. Cyclic voltammograms of Ni(OH)₂ material deposited on a GC electrode recorded in different electrolytes with a total OH⁻ concentration of 6.5 M. Measurements were performed using an RDE setup with a rotation speed of 1600 rpm and the voltammograms were recorded at scan rate of 20 mV s⁻¹. Five cycles were performed, and the figure shows the third cycle for all electrolyte compositions. The currents are normalized by milligrams of Ni(OH)₂ electrocatalyst present for the sake of comparison.

of the electrolyte composition on both the battery and the electrolyser functionalities of the nickel hydroxide electrode. The peak potentials for both Ni(OH)₂ oxidation and NiOOH reduction are used to determine the effect of adding specific alkali metal cations on the battery functionality, as these potentials are key performance indicators for the charging and the discharging reactions. This is due to the fact that a decrease in the potential difference between the Ni(OH)₂ oxidation and NiOOH reduction peak potential indicates a higher voltaic efficiency for the battery functionality.

In Fig. 1 we see that the addition of different alkali metal cations has different effects on the Ni(OH)₂/NiOOH redox potentials. In the presence of Li⁺ and Rb⁺ a lower oxidation potential is observed, with respect to a pure KOH electrolyte, while the highest reduction potentials are observed in the presence of Li⁺, Rb⁺ and in a pure KOH electrolyte.

To investigate the effect of alkali metal cation additions on the OER activity in concentrated hydroxide electrolytes, we compare the potential necessary to reach a current density of 200 mA/mg. In Fig. 1 we can clearly observe that these potentials are dependent on the presence of the alkali cations in the electrolyte. In these highly concentrated electrolytes the trend for OER activity, comparing the potential necessary to reach 200 mA/mg, is Rb⁺ > Cs⁺ > Na⁺ > Li⁺. It is important to note that the majority of the electrolyte for all these experiments is composed of KOH, and only a fraction of the cations present stem from the MOH additions. The trend we observe in concentrated solutions is similar than the trends observed in low concentration electrolytes, where the trend for OER activity is reported to be Cs⁺ > Na⁺ > K⁺ > Li⁺ [30].

A summary of the CV characteristics, including peak oxidation and reduction potential and OER potential of all the alkali metal cation concentrations tested is shown in Fig. 2. To improve battery functionality the peak oxidation potential (purple) should be as low as possible, and the peak reduction potential (green) should be as high as possible. This will result in the lowest charging potential and the highest discharging potential. To increase gas production, the potential at which OER happens (blue) should be as low as possible.

The mixture with the most favorable onset potential for OER is 1 M of RbOH and 5.5 M KOH. The addition of Rb⁺ shows a proportional trend in the peak oxidation and reduction potentials of Ni(OH)₂/NiOOH and OER potential with respect to concentration, meaning that an increase in Rb⁺ concentration will result in an increase in the potential at which the discharging reaction takes place and a decrease in the potentials of the charging reaction and OER. For Li⁺ mixtures a similar trend is observed

Table 2
Battery cycling test steps and details.

| Test phase | Electrolyte Details | Number of cycles |
|------------|-------------------------------------|------------------|
| 1 | 5 M KOH | 30 |
| 2 | 6.5 M OH ⁻ concentration | 30 |
| 3 | 5 M KOH | 30 |

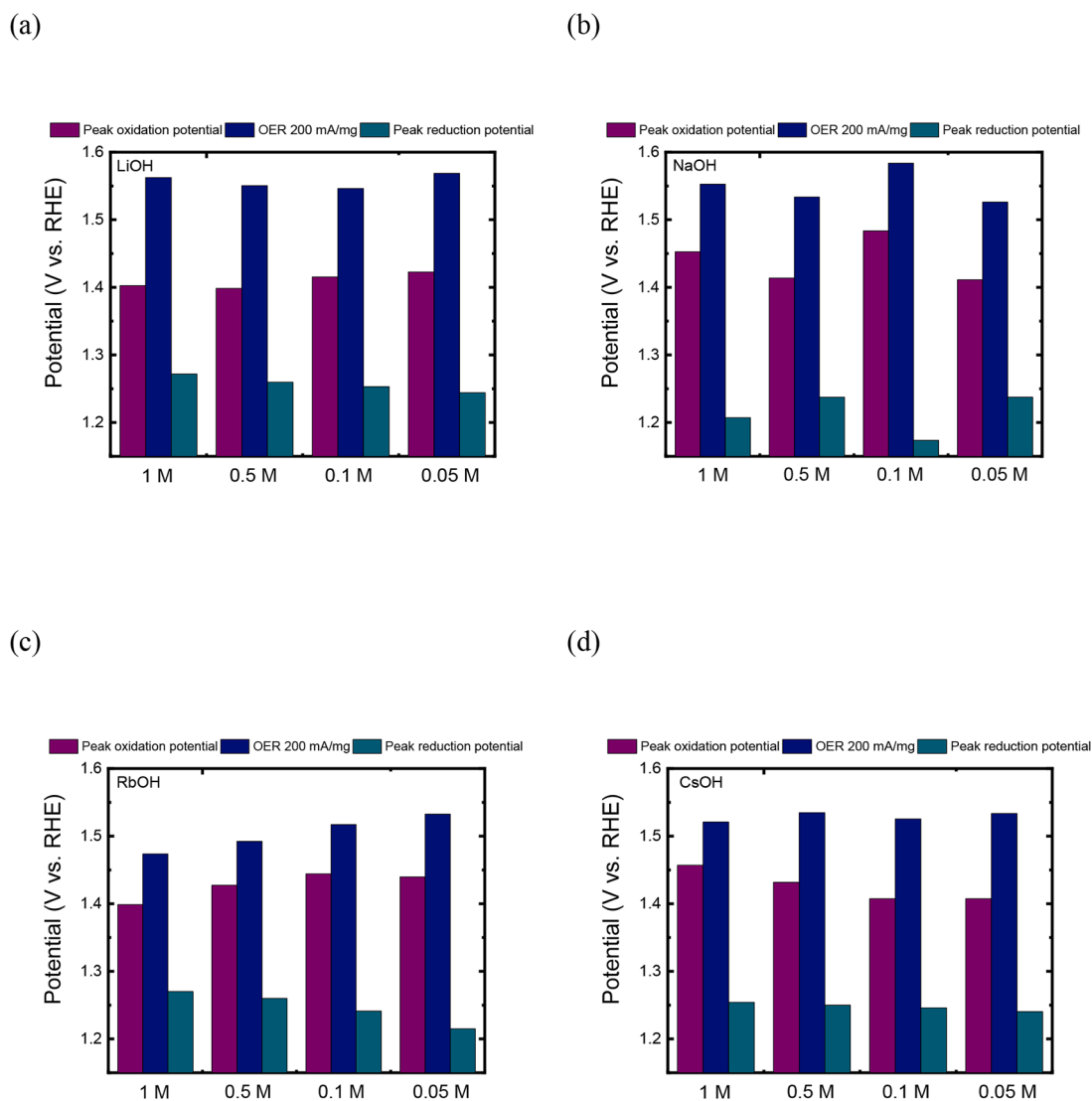


Fig. 2. Peak oxidation (purple) and reduction (green) potential of the $\text{Ni}(\text{OH})_2/\text{NiOOH}$ redox couple and the potential at which 200 mA/mg for OER (blue) is reached for different electrolyte compositions. (a) LiOH, (b) NaOH, (c) RbOH, and (d) CsOH additions to a KOH electrolyte. Data from cyclic voltammograms of a $\text{Ni}(\text{OH})_2$ film deposited on a GC-RDE at 1600 rpm.

for the peak oxidation and reduction potentials of $\text{Ni}(\text{OH})_2/\text{NiOOH}$, however the OER potentials remains rather constant at different Li^+ concentrations. The OER potentials for the Li^+ mixtures are the highest in comparison to the mixtures with other alkali cation mixtures, indicating that Li^+ additions have a negative effect on the OER activity of the

NiOOH electrode. This is in agreement with earlier work in low concentration hydroxide electrolytes [30]. The increase in concentration of Na^+ does not result in a proportional difference in the redox potentials or OER potential. For CsOH additions an increase in the peak oxidation potential is observed with increasing Cs^+ concentrations, while both the peak reduction potential and OER potential are relatively constant and are not affected by the concentration of CsOH added.

Overall, the data shows how the addition of different concentrations of alkali metal cations can be used to tune the reactions happening, both for the battery functionality and the electrolysis functionality of a nickel electrode. In an integrated device the modification of the electrolyte composition can be used to alter the ratio of the different products, battery storage and hydrogen production. Taking the results of Fig. 2 into account, LiOH, RbOH, and CsOH additions seem to be the most suitable to integrate both technologies, because they allow for a higher voltaic battery efficiency, and depending on the alkali metal cation

concentration, can also result in a lower potential for the OER, depending on the concentration.

It is reported that the α/γ phases of $\text{Ni}(\text{OH})_2/\text{NiOOH}$ have a higher onset potential for OER [22,31–33]. It is therefore possible that the Li^+ cations can intercalate in the nickel layered hydroxide structure and stabilize the α/γ phases. This could further explain the difference in the catalytic activity of OER reported by Garcia et al. [20], where there is a different behavior at higher potentials with Li^+ and K^+ electrolyte than with Cs^+ and Na^+ at low concentrations. In their results this is shown in a different slope during LSVs with the different cations, where Li^+ and K^+ behave differently than Cs^+ and Na^+ . In highly concentrated, pure KOH electrolytes, Cappadonia et al. found that $\beta\text{-Ni}(\text{OH})_2$ is more stable than $\alpha\text{-Ni}(\text{OH})_2$, and that the α phase will transform into the β phase over time [32]. We believe that the presence of specific alkali metal cations, namely Li^+ because of its smaller size, can stabilize the α/γ phase in highly alkaline electrolyte solutions. Even small additions of Li^+ result in a consistently modified electrochemical behavior. The resulting lower OER activity coincides with the stabilization of α/γ phases of $\text{Ni}(\text{OH})_2/\text{NiOOH}$, where Li^+ additions result in a higher onset potential for OER.

Although the RDE experiments provide information on both the

battery and the electrolyser functionalities, the amount of material on the surface is small. Therefore, to test the long-term effects of alkali metal cation additions and to better mimic the effects on the integration of both electrolysis and battery charging/discharging reactions, further experiments were performed in battery setups to determine whether these effects are also observed during longer time battery cycling experiments.

3.2. Battery cycling

To compare the results of long-term battery cycling experiments, the discharge capacity of each battery cycle has been calculated. First, the batteries electrodes were conditioned for 30 cycles in 5 M KOH. Then, 30 additional charging/discharging cycles were run with the electrolytes detailed in Table 1. Finally, 30 cycles in 5 M KOH were run after the cycles with electrolyte mixtures to determine if the effect of the alkali metal cation is only present when the cation is present in the electrolyte solution. The last cycle (cycle number 30) of each step in the protocol is shown in the SI Fig. S.2 for all 16 batteries. Changes in the battery capacity after the charging/discharging cycles in a 5 M KOH electrolyte and in the electrolyte mixtures are shown in Fig. 3. The discharge capacity of each battery in the last cycle of the activation phase was used as a reference point and the discharge capacity of each battery in the relevant electrolyte was compared to the reference point. All changes in the battery capacity are given as percentages. Increasing the

concentration of both Li^+ and Rb^+ leads to lower increases in battery capacity. For Cs^+ mixtures this is not the case as the battery capacity remains constant with 0.05 M Cs^+ in the electrolyte and increases only with higher Cs^+ concentrations. The findings of the battery tests coincide with the findings of the RDE experiments where Li^+ presented a low peak oxidation potential and a high peak reduction potential, together with a lower OER activity.

Only with the addition of LiOH, in all concentrations except the lowest (0.05 M LiOH + 6.45 M KOH), does the capacity not decrease after flushing the batteries and replacing the electrolyte by a pure KOH solution. This indicates that the addition of LiOH in the electrolyte brings about a permanent change in the electrode materials. The effect of the Li^+ addition can be seen up to 30 cycles after it is removed from the electrolyte. Thereby, Li^+ additions improve the battery capacity even after the Li^+ has been removed from the electrolyte. Although some of the other cations have a positive effects on the battery discharge capacity, this is only the case with the cation present in the electrolyte. For the other cations, in particular Rb^+ and Cs^+ , the increased battery capacity starts to lower in the first cycle where the electrolyte is changed, but drops off considerably after approximately 20 cycles.

There is little information on the effect of Li^+ in NiFe batteries reported in literature. Lei et al. report that the use of LiOH in KOH electrolyte enhances the dissolution of iron in the electrolyte, therefore increasing Fe crossover in the battery cell. They attribute this increased capacity to the formation of porous iron structures in the negative

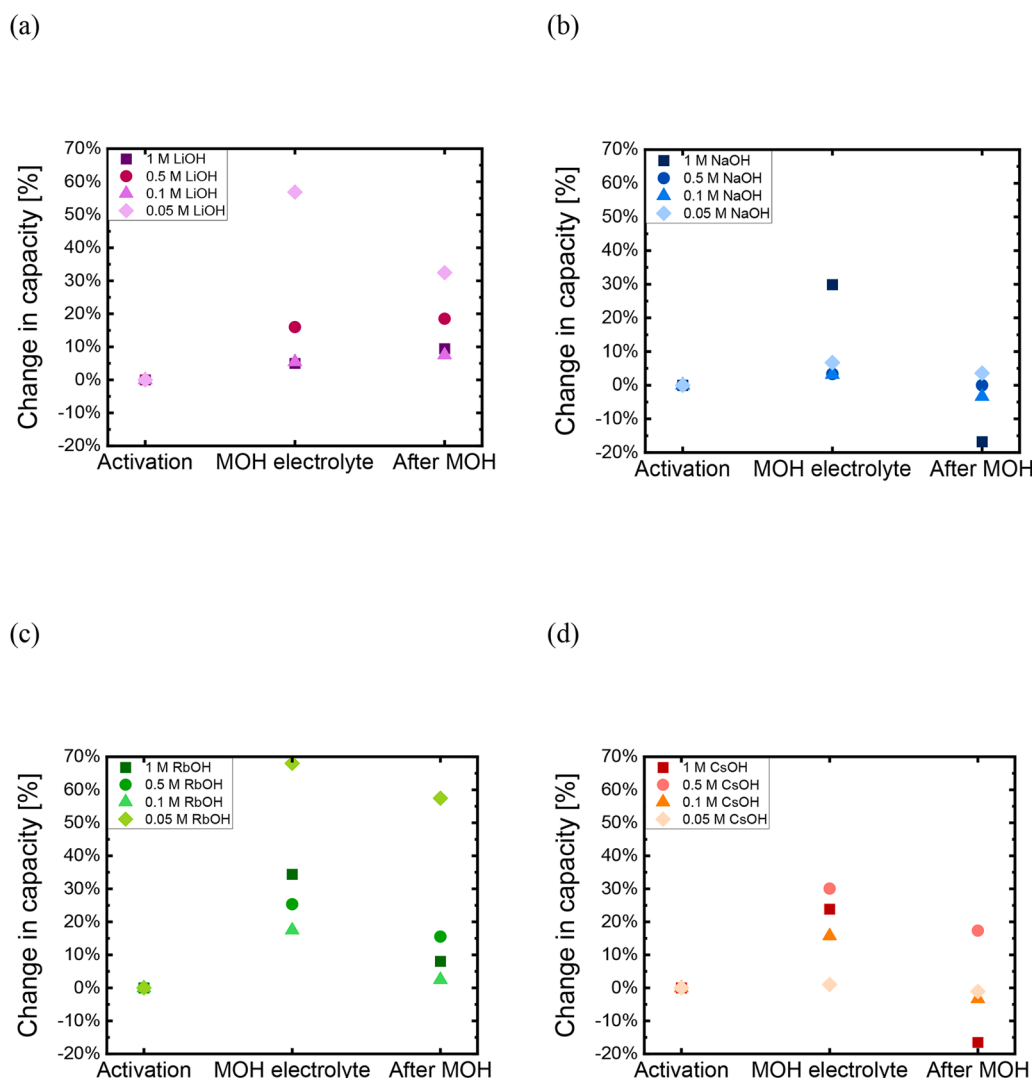


Fig. 3. Changes in the discharge capacity after 30 subsequent charging/discharging cycles in 5 M KOH (activation), electrolyte mixtures (MOH electrolyte) and 5 M KOH (after MOH). The discharge capacity of the last cycle of each phase is calculated and compared to the capacity after activation of each individual battery. Changes in the discharge capacity are displayed as percentages with respect to the activation phase as references. The figures shows electrolytes containing: (a) LiOH, (b) NaOH, (c) RbOH, and (d) CsOH additions to a KOH electrolyte.

electrode due to Li^+ incorporation [34]. Posada and Hall also report an increase in the performance of the battery with the addition of LiOH [35]. Hills confirms that an increase in the efficiency of the nickel oxide electrode is the cause of the enhanced performance in batteries containing LiOH in the electrolyte, possibly due to a change in the conductivity [36]. Here we have shown that the addition of Li^+ brings about a permanent change in the capacity of the nickel electrode. This is a strong indication that Li^+ is intercalated into the nickel electrode, stabilizing the α/γ phases that have higher average oxidation states.

It has been shown that the standard electrode potentials of the Ni (OH)₂/NiOOH redox couple can shift due to the organization of the lattice structure in both α/γ and β/β systems [22]. Therefore, it is possible that by including the cations in long-term cycling of the battery, the lattice parameters are stabilized and organized in a specific way. The γ -NiOOH phase has a larger interspatial sheet distance due to the presence of additional water and alkali metal cations. Furthermore, it has a higher average oxidation state, which would explain the larger battery capacity obtained. It is reported that the uptake of alkali metal cations is expected in the γ -NiOOH phase and not in the β -NiOOH phase [22]. Therefore, by adding a small percentage of LiOH to the KOH electrolyte the α/γ phase is stabilized resulting in a higher battery capacity. As shown by the RDE experiments the stabilization of this phase does not significantly increase the potential at which oxygen is evolved. Our results indicate that there is an optimal cation concentration for the stabilization of the α/γ phase, leading to concentration dependent increases in battery capacity. The interaction of Li^+ with the NiOOH phases is strong, as the addition of Li^+ brings about a permanent change in the electrode, indicating that Li^+ is not leached out of the electrode during charging/discharging cycles.

3.3. Battolyser electrolyte optimization

Since the battolyser functions as both a battery and an electrolyser it is also important to investigate the potential at which water electrolysis takes place with the addition of these cations. For optimizing a hybrid application, such as the battolyser, positive effects on the battery capacity can be counteracted by an increase in the potential for water splitting, as the energy efficiency of the application is dependent on both functionalities. To determine the cell potential at which water electrolysis occurs in the integrated device, the last 5 cycles of the experiments with different MOH concentrations added to the KOH electrolyte are taken into account. The highest potential of the charging plateau

from the last 5 cycles are averaged to determine the average potential at which gas evolution happens. Fig. 4 indicates the average cell potentials at which water electrolysis occurs, and the error bars indicate the deviation of these values over the last 5 cycles.

The data in Fig. 4 indicates that for high concentrations of LiOH and NaOH (1 M and 0.5 M Li^+ , 1 M Na^+) the potential for gas evolution is indeed significantly higher than that for pure KOH. The decrease in potential with decreasing MOH concentration is very closely related to the increase in the overall conductivity of the electrolyte, the electrolyte mixture had a 6.5 M MOH concentration while the benchmark is a 5 M KOH electrolyte used for the activation cycles. Therefore, we mainly observe that the gas evolution functionality increases when the conductivity of the solution results in a decreased gas evolution potential.

With regards to electrolyser functionality and optimizing the amount of hydrogen produced, we look to reduce the cell potential for gas evolution. Therefore, in this case, taking into account the data from RDE and battery cycling, the lower concentrations of alkali metal cation additions are beneficial. Regarding the NiFe battery functionality and the widespread use of LiOH in high concentrations, we have shown that the Li^+ additions increase battery capacity and in high concentrations will increase the onset potential for gas evolution. Therefore, to optimize the battery functionality high concentrations of LiOH are beneficial.

For the integrated device it is important to optimize including the trade-offs of the combined effects. Therefore, LiOH additions seem promising, since they result in higher battery capacity. These additions should be kept in the low concentrations, as increasing the LiOH will only decrease the electrolyte conductivity and will result in a higher onset potential for gas evolution. In this way, both functionalities can be integrated and the battolyser device can combine both battery and electrolysis functionalities. Interestingly, 0.05 M RbOH additions also display a large increase in the battery capacity, even surpassing the effect of LiOH additions. The cell potential necessary for gas evolutions with a 0.05 M RbOH addition is however slightly higher than the cell potential with a 0.05 M LiOH addition. This indicates that these RbOH additions are preferred when optimizing for battery capacity, while LiOH additions are preferred when optimizing for gas evolution. It should be noted however that Li^+ additions will be less costly than Rb^+ additions if used for larger scale applications. Overall, we conclude that the electrolytes that should be used to provide optimum energy efficiencies for this integrated device are either a 0.05 M LiOH + 6.45 M KOH electrolyte or a 0.05 M RbOH + 6.45 M KOH electrolyte, since these will result in the highest battery capacity and the lowest cell potential for gas evolution.

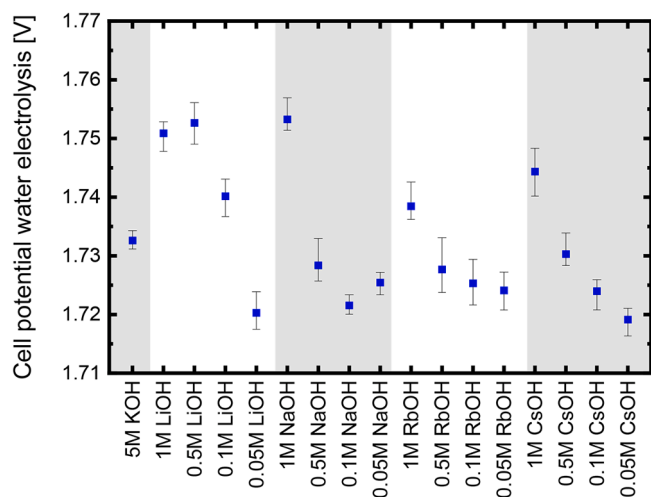


Fig. 4. Cell potentials at which gas evolution (H_2 and O_2 evolution) occurs after full charging NiFe batteries for 17 different electrolyte compositions at a 2 A charging current. Average values of 5 cycles are presented, where the error bars indicate the maximum and minimum values of the 5 last cycles.

4. Conclusions

Here, we have investigated the effect of alkali hydroxide additions to concentrated KOH electrolytes on the OER performance and battery capacity of nickel electrodes. We show that the addition of different metal alkali cations has an effect on the electrochemical performance of the nickel electrode, both with regards to battery capacity and OER activity. For OER activity, the trend found during RDE setup experiments in high concentration hydroxide electrolytes is $\text{Rb}^+ > \text{Cs}^+ > \text{K}^+ > \text{Na}^+ > \text{Li}^+$. This is possibly due to the size effect of the different cations, as smaller cations, such as Li^+ , can intercalate in the NiOOH-LDH and stabilize the γ -NiOOH phase. This results in a higher onset potential for OER. For the larger cations, Rb^+ and Cs^+ , we find that only large additions (of 1 M or 0.5 M) cause a significant decrease in OER potential. The intercalation of small cations also causes an increase in battery electrode capacity because of the higher average valence of the Ni (OH)₂/NiOOH α/γ pair. Small concentrations of Li^+ added to a concentrated KOH electrolyte can therefore be beneficial for the nickel electrode battery functionality and for an integrated battery and electrolyser system, where it increases the battery capacity without a significant increase in OER onset potential. Further experiments with NiFe

batteries at longer time scales show that the effect of lithium inclusions in the nickel electrode are still present in the battery capacity for at least 30 cycles after the electrolyte has been changed to pure KOH. For an integrated device, with both battery and electrolyser functionality, we find that the optimum electrolytes are either a 0.05 M LiOH + 6.45 M KOH electrolyte or a 0.05 M RbOH + 6.45 M KOH electrolyte, as these result in a higher battery capacity and lowest cell potentials for gas evolution.

CRedit authorship contribution statement

A. Mangel Raventos: Methodology, Investigation, Visualization, Data curation, Project administration, Writing – original draft, Writing – review & editing. **R. Kortlever:** Data curation, Writing – review & editing, Conceptualization, Supervision.

Declaration of Competing Interest

The authors declare that they have no known competing financial interests or personal relationships that could have appeared to influence the work reported in this paper.

Acknowledgements

The authors would like to acknowledge Michel van den Brink for performing ICP-OES measurements and Simone Asperti for SEM images.

Supplementary materials

Supplementary material associated with this article can be found, in the online version, at [doi:10.1016/j.electacta.2022.140255](https://doi.org/10.1016/j.electacta.2022.140255).

References

- M.D. Leonard, E.E. Michaelides, D.N. Michaelides, Energy storage needs for the substitution of fossil fuel power plants with renewables, *Renew. Energy* 145 (2020) 951–962, <https://doi.org/10.1016/j.renene.2019.06.066>.
- T. Tsoutsos, N. Frantzeskaki, V. Gekas, Environmental impacts from the solar energy technologies, *Energy Policy* 33 (2005) 289–296, [https://doi.org/10.1016/S0301-4215\(03\)00241-6](https://doi.org/10.1016/S0301-4215(03)00241-6).
- G. Coppez, S. Chowdhury, S.P. Chowdhury, The importance of energy storage in renewable power generation: a review, in: *Proceedings of the Universities Power Engineering Conference*, 2010.
- S. Badwal, S.S. Giddey, C. Munnings, A.I. Bhatt, A.F. Hollenkamp, Emerging electrochemical energy conversion and storage technologies, *Front. Chem.* 2 (2014) 1–28, <https://doi.org/10.3389/fchem.2014.00079>.
- S.C. Mueller, P.G. Sandner, I.M. Welp, Monitoring innovation in electrochemical energy storage technologies: a patent-based approach, *Appl. Energy* 137 (2015) 537–544, <https://doi.org/10.1016/j.apenergy.2014.06.082>.
- Z. Yang, et al., Electrochemical energy storage for green grid, *Chem. Rev.* 111 (5) (2011) 3577–3613, <https://doi.org/10.1021/cr100290v>.
- F.M. Mulder, B.M.H. Weninger, J. Middelkoop, F.G.B. Ooms, H. Schreuders, Efficient electricity storage with a battery, an integrated Ni-Fe battery and electrolyser, *Energy Environ. Sci.* 10 (2017) 756–764, <https://doi.org/10.1039/c6ee02923j>.
- F.M. Mulder, Implications of diurnal and seasonal variations in renewable energy generation for large scale energy storage, *J. Renew. Sustain. Energy* 6 (3) (2014), <https://doi.org/10.1063/1.4874845>.
- A.J. Salkind, *Alkaline Storage Batteries*, Wiley, New York, 1969.
- B. Hariprakash, S.K. Martha, M.S. Hegde, A.K. Shukla, A sealed, starved-electrolyte nickel-iron battery, *J. Appl. Electrochem.* 35 (1) (2005) 27–32, <https://doi.org/10.1007/s10800-004-2052-y>.
- A. Ursua, P. Sanchis, L.M. Gandia, Hydrogen production from water electrolysis: current status and future trends, *Proc. IEEE* 100 (2) (2012) 410–426.
- D. Zhou, et al., Effects of redox-active interlayer anions on the oxygen evolution reactivity of NiFe-layered double hydroxide nanosheets, *Nano Res.* 11 (3) (2018) 1358–1368, <https://doi.org/10.1007/s12274-017-1750-9>.
- B.J. Trześniewski, et al., *In situ* observation of active oxygen species in Fe-containing Ni-based oxygen evolution catalysts: the effect of pH on electrochemical activity, *J. Am. Chem. Soc.* 137 (48) (2015) 15112–15121, <https://doi.org/10.1021/jacs.5b06814>.
- O. Diaz-Morales, D. Ferrus-Suspedra, M.T.M. Koper, The importance of nickel oxyhydroxide deprotonation on its activity towards electrochemical water oxidation, *Chem. Sci.* 7 (4) (2016) 2639–2645, <https://doi.org/10.1039/c5sc04486c>.
- I.C. Faria, R. Torresi, A. Gorenstein, Electrochemical intercalation in NiOx thin films, *Electrochim. Acta* 38 (18) (1993) 2765–2771, [https://doi.org/10.1016/0013-4686\(93\)85096-H](https://doi.org/10.1016/0013-4686(93)85096-H).
- M. Wehrens-Dijkstra, P.H.L. Notten, Electrochemical quartz microbalance characterization of Ni(OH)₂-based thin film electrodes, *Electrochim. Acta* 51 (18) (2006) 3609–3621, <https://doi.org/10.1016/j.electacta.2005.10.022>.
- D.M. Constantin, E.M. Rus, L. Oniciu, L. Ghergari, The influence of some additives on the electrochemical behaviour of sintered nickel electrodes in alkaline electrolyte, *J. Power Sources* 74 (2) (1998) 188–197, [https://doi.org/10.1016/S0378-7753\(98\)00053-6](https://doi.org/10.1016/S0378-7753(98)00053-6).
- J.D. Michael, E.L. Demeter, S.M. Illes, Q. Fan, J.R. Boes, J.R. Kitchin, Alkaline electrolyte and Fe impurity effects on the performance and active-phase structure of NiOOH thin films for OER catalysis applications, *J. Phys. Chem. C* 119 (21) (2015) 11475–11481, <https://doi.org/10.1021/acs.jpcc.5b02458>.
- J. Zaffran, et al., Influence of electrolyte cations on Ni(Fe)OOH catalyzed oxygen evolution reaction, *Chem. Mater.* 29 (11) (2017) 4761–4767, <https://doi.org/10.1021/acs.chemmater.7b00517>.
- A.C. Garcia, T. Touzalim, C. Nieuwland, N. Perini, M.T.M. Koper, Enhancement of oxygen evolution activity of NiOOH by electrolyte alkali cations, *Angew. Chem. Int. Ed.* 58 (37) (2019) 12999–13003, <https://doi.org/10.1002/anie.201905501>.
- T.B. Reddy, D. Linden, *Handbook of Batteries*, 3rd ed., McGraw-Hill, New York, 2002.
- R. Barnard, C.F. Randell, F.L. Type, Studies concerning charged nickel hydroxide electrodes. I. Measurement of reversible potentials, *J. Appl. Electrochem.* 10 (1980) 109–125.
- L. Trotochaud, S.L. Young, J.K. Ranney, S.W. Boettcher, Nickel-iron oxyhydroxide oxygen-evolution electrocatalysts: the role of intentional and incidental iron incorporation, *J. Am. Chem. Soc.* 136 (18) (2014) 6744–6753, <https://doi.org/10.1021/ja502379c>.
- P. Oliva, et al., Review of the structure and the electrochemistry of nickel hydroxides and oxy-hydroxides, *J. Power Sources* 8 (2) (1982) 229–255, [https://doi.org/10.1016/0378-7753\(82\)80057-8](https://doi.org/10.1016/0378-7753(82)80057-8).
- M.W. Louie, A.T. Bell, An investigation of thin-film Ni-Fe oxide catalysts for the electrochemical evolution of oxygen, *J. Am. Chem. Soc.* 135 (33) (2013) 12329–12337, <https://doi.org/10.1021/ja405351s>.
- A. Irazzo, F.M. Mulder, Nickel-iron layered double hydroxides for an improved Ni/Fe hybrid battery-electrolyser, *Cite this, Mater. Adv.* 2 (2021) 5076, <https://doi.org/10.1039/d1ma00024a>.
- S. Jung, C.C.L. McCrory, I.M. Ferrer, J.C. Peters, T.F. Jaramillo, Benchmarking nanoparticulate metal oxide electrocatalysts for the alkaline water oxidation reaction, *J. Mater. Chem. A* 4 (8) (2016) 3068–3076, <https://doi.org/10.1039/c5ta07586f>.
- T. Reier, M. Oezaslan, P. Strasser, Electrocatalytic oxygen evolution reaction (OER) on Ru, Ir, and Pt catalysts: a comparative study of nanoparticles and bulk materials, *ACS Catal.* 2 (8) (2012) 1765–1772, <https://doi.org/10.1021/cs3003098>.
- C.C.L. McCrory, S. Jung, I.M. Ferrer, S.M. Chatman, J.C. Peters, T.F. Jaramillo, Benchmarking hydrogen evolving reaction and oxygen evolving reaction electrocatalysts for solar water splitting devices, *J. Am. Chem. Soc.* 137 (13) (2015) 4347–4357, https://doi.org/10.1021/JA510442P/SUPPL_FILE/JA510442P_SI_001_Apr.PDF.
- A.C. Garcia, T. Touzalim, C. Nieuwland, N. Perini, M.T.M. Koper, Enhancement of oxygen evolution activity of nickel oxyhydroxide by electrolyte alkali cations, *Angew. Chem. Int. Ed.* 58 (37) (2019) 12999–13003, <https://doi.org/10.1002/anie.201905501>.
- B.S. Yeo, A.T. Bell, *In situ* Raman study of nickel oxide and gold-supported nickel oxide catalysts for the electrochemical evolution of oxygen, *J. Phys. Chem. C* 116 (15) (2012) 8394–8400, <https://doi.org/10.1021/jp3007415>.
- M. Cappadonia, J. Divisek, T. von der Heyden, U. Stimming, Oxygen evolution at nickel anodes in concentrated alkaline solution, *Electrochim. Acta* 39 (11/12) (1994) 1559–1564.
- D.J. Lockwood, D.S. Hall, C. Bock, B.R. Macdougall, Nickel hydroxides and related materials: a review of their structures, synthesis and properties, *Proc. R. Soc. A Math. Phys. Eng. Sci.* 471 (2014), <https://doi.org/10.1098/rspa.2014.0792>.
- D. Lei, D.C. Lee, A. Magasinski, E. Zhao, D. Steingart, G. Yushin, Performance enhancement and side reactions in rechargeable nickel-iron batteries with nanostructured electrodes, *ACS Appl. Mater. Interfaces* 8 (3) (2016) 2088–2096, <https://doi.org/10.1021/acsami.5b10547>.
- J.O.G. Posada, P.J. Hall, The effect of electrolyte additives on the performance of iron based anodes for NiFe cells, *J. Electrochem. Soc.* 162 (10) (2015) A2036–A2043, <https://doi.org/10.1149/2.0451510jes>.
- S. Hills, Beneficial effect of lithiated electrolyte on iron battery electrodes, *J. Electrochem. Soc.* 112 (10) (1964).